Supplemental Material

Expanded Materials and Methods:

Data Availability: The data that support the findings of this study are available from the corresponding author upon reasonable request. The whole-genome shotgun raw sequence data are available from NCBI Sequence Read Archive under BioProject PRJNA692044 (https://www.ncbi.nlm.nih.gov/sra).

Rats and Housing: All animal protocols were approved by the Institutional Animal Care and Use Committee at Baylor College of Medicine, Houston, TX and conformed to the Guide for the Care and Use of Laboratory Animals, 8th edition, published by the National Institutes of Health (NIH). SHRSP and WKY rats were obtained from Charles Rivers Rats and mated for at least four generations to produce in-house colonies for each strain. Rats were subjected to a 12 h light (6 AM– 6 PM): 12 h dark (6 PM– 6 AM) cycle. In all studies, rats were co-housed with littermates, and all rats in a cage were exposed to the same experimental conditions. A minimum sample size of 6 per group was calculated using SigmaPlot 13 based on previous SBP data with an effect size of 10mmHg, a significance level (alpha) of 0.05, and a power of 0.8. No animals enrolled in the study were excluded from analysis.

EODF Feeding Protocol: At 5 weeks of age, male WKY and SHRSP cages were randomized to *ad libitum* feeding (control) or EODF groups, n=6-8 per group. Only males were studied as SHRSP males exhibit greater SBP elevation as compared to females, allowing increased power of the study to detect improvements by EODF. EODF rats were exposed to alternating 24-hours of *ad libitum* food access followed by 24-hours of no food access. Standard irradiated chow (LabDiet 5V5R, Fort Worth, TX) with 23.1% calories from protein, 14.8% from fat, and 62.1% from carbohydrates was used. Food was removed or replaced between 8 A.M. and 9 A.M. Food intake per day was calculated by weighing the food at the end of a 24-hour period of feeding for all groups and dividing the food eaten by the number of rats in the cage. The body weight of all rats was measured daily. Control and EODF feeding protocol continued for 10 weeks.

Cecal Microbiota Transplant: Cecal content from 3 rats per group were pooled, diluted 1:20 with sterile PBS, centrifuged at 1000 rpm for 5 minutes, aliquoted and frozen at -80°C for future gavage of germ-free rats. Eight-week-old male Swiss Webster germ-free rats were obtained from the Baylor College of Medicine Gnotobiotics Core. Quantitative PCR of the 16S rRNA gene was performed on rat feces from each isolator to confirm germ-free status. Fecal 16S rRNA copy numbers <250/5ng DNA are considered germ-free by the Gnotobiotic Core, samples from isolators used in this study resulted in a mean copy number of 95.5 ± 17.4. Additionally, all isolators tested negative by microscopic

exam of a gram-stained fecal smear as well as aerobic, anaerobic, and fungal culture every two weeks. Immediately upon exiting the germ-free isolation chamber, rats were gavaged with 500µl of cecal content supernatant, which was repeated 24 hours later, n=6-8 per group. Rats were housed in sterile cages with littermates that received cecal transplant from the same donor group and provided *ad libitum* access to sterilized water and irradiated normal chow. Blood pressure was measured every other week beginning at 10 weeks of age. The study was terminated when rats were 20 weeks old, when cecal contents were isolated for microbiota and metabolite measurements.

Cholic Acid Dietary Supplementation: At 6 weeks of age male WKY and SHRSP rats were randomized to vehicle control or CA treatment groups, n=6-8 per group. The control group was fed with a normal diet (Teklad, TD.110180) and the CA supplemented group was fed with an isocaloric diet with 0.5 % CA (Teklad, TD.130107). Previous rodent studies have demonstrated this concentration to activate the BA receptor TGR5 without inducing a hepatic inflammatory response[19,20]. All rats had access to food ad libitum. The dietary treatment continued for 15-16 weeks.

Oleanolic Acid Treatment: At 6 weeks of age male SHRSP rats were randomized to vehicle control or oleanolic acid (OA) treatment groups, n=5-6 per group. OA (10 mg/kg, Cayman Chemical) was administered to SHRSP through daily intraperitoneal (IP) injections. The control group was injected IP with vehicle (10% DMSO, Sigma Aldrich). All rats had access to food ad libitum. The treatment continued for 15 weeks.

Non-Invasive Blood Pressure Measurements: The CODA Volume Pressure Relationship tail-cuff system (Kent Scientific Corporation) was used to measure SBP in unanesthetized rats. SBP measurements were taken weekly at the end of a feeding day for EODF groups. De-identified cage cards were used to blind the investigator performing SBP measurements. A minimum of 10 consecutive readings, without movement artifact, were averaged for each measurement. Previous studies in our lab and others have demonstrated that SBP values obtained using the tail-cuff method are comparable to direct arterial measurements made in the same rat[21].

Assessment of Vascular Function of Mesenteric Arteries: Mesenteric arteries (2nd order) were isolated and used to evaluate endothelium-dependent vasodilation using an isometric tension recording system, as previously described[22]. Mesenteric artery rings (approximately 1 mm) were equilibrated at 37°C in Krebs buffer (composition in mmol/L: 119 NaCl, 4.7 KCl, 1 $MgSO_4$, 1.2 KH_2PO_4, 20 $NaHCO_3$, 5.5 glucose, 2.5 $CaCl_2$ gassed with 5% CO_2 / 20% O_2 / balance N_2 for pH=7.4;) for 40 min, and then adjusted incrementally (0.2 gram per 10 min) to the optimal resting tension of 2 grams. Krebs buffer was refreshed every 20 min. After equilibration, all rings were contracted three times with 40 mM KCl followed by one 60 mM KCl contraction. Then mesenteric artery segments were preconstricted with phenylephrine (10^{-6} M, Sigma Aldrich) before exposure to increasing doses of acetylcholine (10^{-9} - 10^{-6} M, Sigma Aldrich).

Whole-genome Shotgun Sequencing: Cecal content was collected in a sterile tube and snap frozen. Samples were submitted to the Center for Metagenomics and Microbiome Research at Baylor College of Medicine for whole genome shotgun sequencing (WGS). 6-8 samples per group were used. Genomic bacterial DNA (gDNA) extraction methods optimized to maximize the yield of bacterial DNA from specimens while keeping background amplification to a minimum were employed[26,27]. Metagenomic shotgun sequencing was performed on extracted total gDNA on Illumina sequencers using chemistries that yielded paired-end reads. Sequencing reads were derived from raw BCL files which were retrieved from the sequencer and called into fastq sequences by Casava v1.8.3 (Illumina). Raw fastq sequences underwent quality trimming and PhiX Illumina adapter removal using bbduk3 (BBMap version 38.69)[28]. Trimming parameters were set to a kmer length of 19, allowing one mismatch and a min Phredquality score of 20. Reads with a minimum average quality score below 17 and length shorter than 50 bp after trimming were discarded. A custom in-house script was used to remove the host reads from the trimmed fastq sequences for further taxonomic and functional profiling (see *Bioinformatics Analysis*).

16S rRNA Sequencing: Bacterial genomic DNA extraction methods used are adapted from the methods developed for the NIH-Human Microbiome Project[26,27] Briefly, bacterial genomic DNA was extracted using MagAtract PowerSoil DNA kit (Qiagen) following the manufacturer's instructions. Resulting sequences were demultiplexed based on the unique molecular barcodes. The raw data files in binary base call (BCL) format created by the MiSeq run were first converted into FASTQ format and demultiplexed based on the single-index barcodes using the Illumina 'bcl2fastq' software.

16S rRNA qPCR: Extracted DNA concentrations was measured by Qubit (Life Technologies) for subsequent normalization of quantitative PCR results.

Quantitative PCR (qPCR) sample analysis were performed in a QuantStudio DX Real-Time PCR System (Applied Biosystems), using MicroAmp Fast Optical 96-well reaction plates (0.1ml), MicroAmp optical adhesive film (all Applied Biosystems), and Quanta PerfeCta® SYBR Green FastMix, Low Rox PCR Master Mix (Quanta Biosciences). Each reaction contained 5 µl of 2X Master Mix, 5 µg of DNA template, 500 nM of each primer (IDT), and PCR grade water to a final volume of 10 µl. Amplification was comprised of a 10 min initial denaturation/activation step at 95°C, followed by 40 cycles of 95°C for 10 s, 60°C for 30 s, and a fluorescence measurement. Melting curve analysis was performed by monitoring fluorescence throughout incremental increases of temperature from 60°C to 95°C.

The qPCR primers (1369F-1492R)[29] target regions flanking V9 of the 16S rRNA gene. A standard curve was made using a serially diluted plasmid that contains nt 1369 to 1492 of an E. coli 16S rRNA gene. The concentrations of unknowns were calculated from CT

values using the equation generated from plotting the standard curve. Total copies of 16S/mg of cecal content was calculated using the known weight of starting material and concentration of isolated DNA All samples were run in triplicate, including the standard curve, a set of non-template controls (NTC), and inhibitor controls (known positives + unknown DNA).

Untargeted Metabolomics: Cecal content and plasma were collected from 15-week-old rats at the end of a feeding day in sterile tubes and snap frozen. Samples were submitted to Metabolon, Inc. (Morrisville, NC) for untargeted metabolomics. Plasma (100ul) and cecal content (100mg) samples (n=6-8 per group) were homogenized and subjected to methanol extraction. The purified supernatant was divided into aliquots corresponding to the various analytical methodologies, then subsequently evaporated and reconstituted with the appropriate analytical injection solvent. Samples were analyzed with four separate methods: two positive mode methods (Pos Early UHPLC-RP/MS/MS and Pos Late UHPLC-RP/MS/MS) and two negative mode methods (Neg UHPLC-RP/MS/MS and Neg UHPLC HILIC/MS/MS) to ensure broad coverage of biochemicals[30]. Metabolites were identified by automated comparison of ion features to a reference library of chemical standards followed by visual inspection for quality control[31]. For downstream analysis, any missing values were assumed to be below the limits of detection and were imputed with the compound minimum (minimum value imputation). Log 10 transformation was performed prior to statistical analysis.

Plasma BA Measurements: Plasma was submitted to the Metabolomics Core at Baylor College of Medicine for relative BA measurement by HPLC as previously described[23,24]. Data was acquired with Agilent mass hunter acquisition software and analyzed with Mass hunter workstation quantitative software.

Bioinformatic analysis:

Microbial WGS analysis:
For metagenomes, taxonomic and functional profiles were generated using High Performance Computer Cluster (HPCC) of Biomedical Informatics Group at Baylor College of Medicine. Average 58391143 of 75-150 pair-end raw reads were input into KneadDatav0.73 to first filter out rat genome using rn6 database. Average 52081822 decontaminated reads were used for the following process. Taxonomic profiles generated using MetaPhlAn[32]v3.0.2. Functional profiles were constructed by HUMAnN[33] v3.0.0.alpha.3 Sample reads were mapped against a pangenomes database[34] to quantify species-specific gene presence and abundance. A translational search was then performed against a UniRef-based protein sequence catalogue with 70% translated identity threshold[35]. Gene families (UniRef90s) profiles were then grouped into ECs and renormalized by copy-per-million reads (cpm). Functional profile dataset was scaled prior

to statistical analysis using mean and standard deviation using StandardScaler function of Scikit-learn[36].

Microbial 16s analysis:
Reads were de-noised and merged into amplicon sequence variants (ASVs) by DADA2 pipeline in R[37,38]. Taxonomic annotations were also generated against DADA2-formatted training FASTA files derived from SILVA138 Database[39]. ASVs with identical taxonomic assignment were grouped into taxonomic bins. Relative abundance was calculated within samples for taxonomic analysis.

Taxonomic analysis:
Taxonomic alpha diversity (species counts and Shannon Index) and Bray-Curtis dissimilarity were calculated using the R package Vegan[40]. Quantification of variation of alpha diversity were done using two-way ANOVA with robust estimator followed by *post hoc* Mann-Whitney U test[25]. Quantifications of variation explained in figure 3A were calculated using PERMANOVA with the adonis function in R package Vegan[40]. Linear discriminant analysis effect size (LEfSe) was used to identify taxa characterizing differences between two groups[41]. Significant differential abundance was detected using two-way ANOVA with robust estimator followed by *post hoc* Mann-Whitney U test[25].

Metabolomics analysis:
Metabolites were grouped by sub-pathways, and sparse partial least squares discriminant analysis (sPLS-DA) with R package mixOmics[42] was used to characterize the differential metabolomic profiles among groups (see Integrated multi-omics analysis). Permutation test with R package RVAideMemoire was used to test for significant differences. Random forest (RF) with Python package Scikit-learn[36]v0.21.3 was used to calculate importance of individual metabolites. RF models were built using 70% of the dataset. Accuracies for RF models were determined by five-fold cross-validation using whole datasets and were 100% and 88.7% for plasma and cecal metabolites respectively. Metabolites with significantly different relative abundances among groups were then grouped by subpathway for visualization (Fig. 4C).

Integrated multi-omics analysis:
Multiple omics data were integrated using a multivariate dimension reduction method DIABLO (Data Integration Analysis for Biomarker discovery using a Latent component method for Omics) from R package mixOmics[42]. Taxonomic and functional profiles were normalized using mean and standard deviation using StandardScaler function of Scikit-learn[36]. Metabolites were normalized by log10 transformation. A tuning process was performed to determine optimal numbers of predictors from each dataset. Minimum misclassification rate and model performance was evaluated by five-fold cross-validation.

Quantitative Real-time PCR Analysis: RNA was isolated from gut sections using the RNeasy Lipid Tissue Mini Kit (Invitrogen), following the manufacturers protocol. RNA was isolated from kidney and brain using TRIzol reagent (Ambion), following the manufacturers protocol. Gene expression was measured quantitative PCR using SYBR Green. Hypoxanthine phosphoribosyltransferase 1 (*Hprt*) was used as the housekeeping gene. Primer sequences are presented in Online Table I.

Histological Analysis: Cecum segments were isolated and fixed in Carnoy's solution, embedded in paraffin and serially sectioned to 4 μm sections. Using manufacturers protocols, sections were stained with hematoxylin and eosin (H&E; Richard Allen Scientific) for intestine architecture or Periodic Acid-Schiff's-Alcian blue (PAS-AB; Sigma Aldrich) for goblet cells enumeration by bright field microscopy (Nikon Eclipse 90i). Crypt height was not different between groups (data not shown). Number of goblet cells per crypt were counted and the average of 15 crypts per cecum was calculated.

Statistical analysis: All data is presented as mean ± SEM unless otherwise noted. The Shapiro-Wilk test was used to assess the normality of distribution of data. Parametric tests were used for normally distributed data sets, including ordinary two-way ANOVA, three-way ANOVA, and student t-test, and non-parametric tests used for non-normally distributed data sets, including Mann-Whitney U test, Kruskal-Wallis test, and two-way ANOVA with robust estimator[25]. Statistical analysis, sample sizes, and p values can be found in the figure or figure legend. All statistics were performed in R or GraphPad Prism 9. Differences were considered statistically significant if $P \leq 0.05$.

Gene name	Species	Primers (5’ -3’)
Muc2	Rat	Forward: 5’- ACCACCATTACCACCACCTCAG -3’
		Reverse: 5’- CGATCACCACCATTGCCACTG -3’
Tlr2	Rat	Forward: 5’- TGGAGGTCTCCAGGTCAAATCT -3’
		Reverse: 5’- TGTTTGCTGTGAGTCCCGAG -3’
Tlr4	Rat	Forward: 5’- GGATTTATCCAGGTGTGAAATTGAG -3’
		Reverse: 5’- TCCACAGCCACCAGATTCTC -3’
Tnfα	Rat	Forward: 5’- AAATGGGCTCCCTCTCATCAGTTC -3’
		Reverse: 5’- TCTGCTTGGTGGTTTGCTACGAC -3’
Il1α	Rat	Forward: 5’- AAGACAAGCCTGTGTTGCTGAAGG -3’
		Reverse: 5’- TCCCAGAAGAAAATGAGGTCGGTC -3’
Il1β	Rat	Forward: 5’- ATCTGGGATCCTCTCCAGTCA -3’
		Reverse: 5’- AGGGCTTGGAAGCAATCCTTAATC -3’
Il17	Rat	Forward: 5’- CTTCACCTTGGACTCTGAGC -3’
		Reverse: 5’- TGGCGGACAATAGAGGAAAC -3’
Cypba	Rat	Forward: 5’- CTTGGGTTTAGGCTCAATGG -3’
		Reverse: 5’- GCGGTGTGGACAGAAGTACC-3’
Ncf1	Rat	Forward: 5’- TGGATTGTCCTTTGAGTCAGG -3’
		Reverse: 5’- CCCAGCGACAGATTAGAAGC -3’
Tjp1	Rat	Forward: 5’- CTTGCCACACTGTGACCCTA -3’
		Reverse: 5’- GGGGCATGCTCACTAACCTT -3’
Il6	Rat	Forward: 5’- TCCTACCCCAACTTCCAATGCTC -3’
		Reverse: 5’- TTGGATGGTCTTGGTCCTTAGCC -3’
Ccl2	Rat	Forward: 5’- TATGCAGGTCTCTGTCACGC -3’
		Reverse: 5’- GGCATTAACTGCATCTGGTG -3’
Cldn4	Rat	Forward: 5’- TGTCTGGGTACGACAGTGGA -3’
		Reverse: 5’- GTAACGTGGAGGCGAGAGAG -3’
Hprt	Rat	Forward: 5’- GCAGTACAGCCCCAAAATGG -3’
		Reverse: 5’- ATCCAACAAAGTCTGGCCTGT-3’

Online Table I. qRT-PCR Primers. All primers were used at a working concentration of 500 nM and an annealing temperature of 60 ˚C.

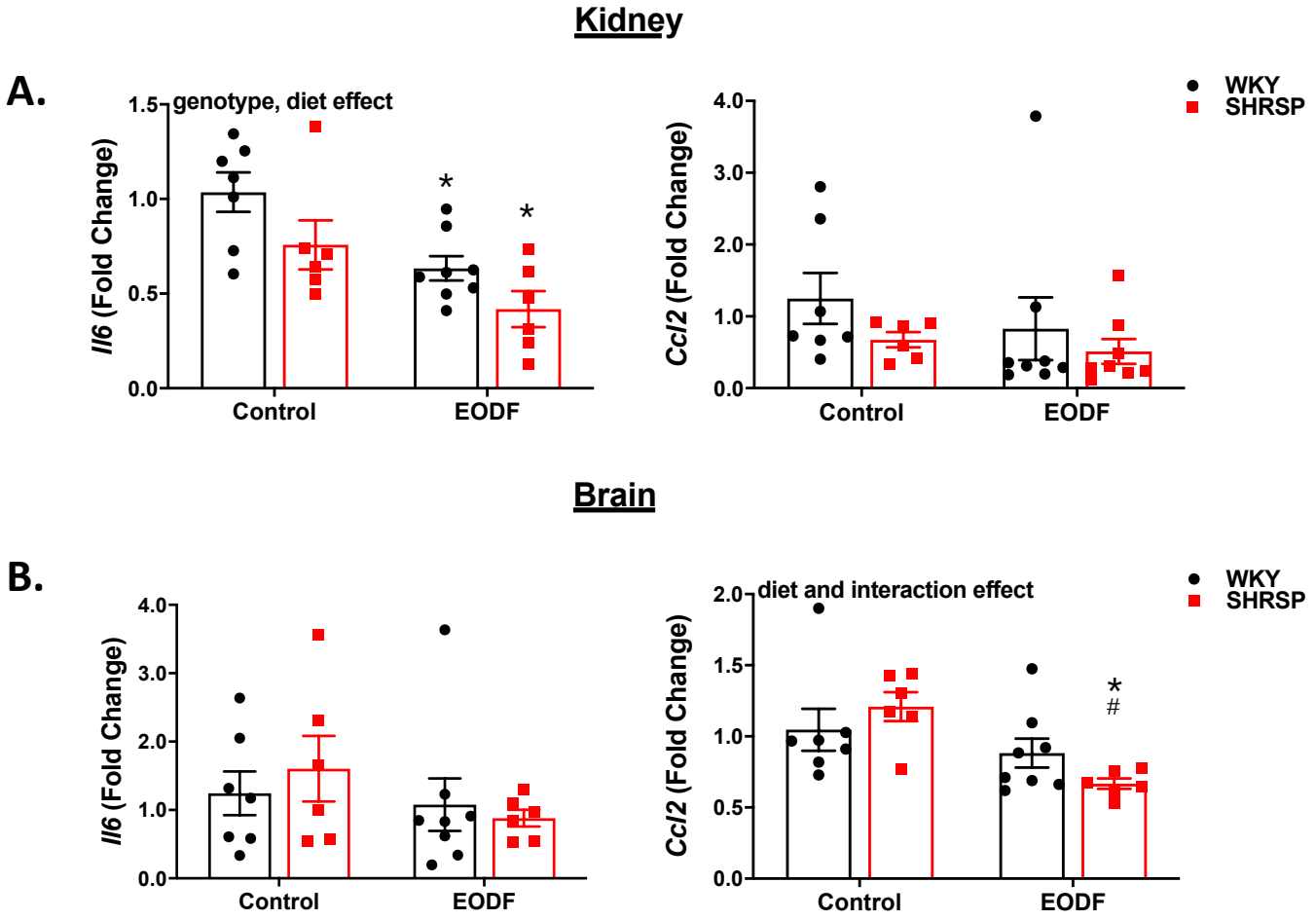

Online Figure I. Markers of inflammation in kidney and brain. Gene expression of *Il6* and *Ccl2* in kidney **(a)** and brain **(b)**. All genes normalized to *Hprt* expression. Two-way ANOVA with robust estimator followed by Mann-Whitney U test with Benjamin-Hochberg *post hoc* correction. Main effect of genotype p=0.0234, diet p=0.0033 for kidney *Il6*, and main effect of diet p=0.01, interaction=0.025 for brain *Ccl2*. *p≤0.05 vs WKY Con, #p≤0.05 vs SHRSP Con. n=6-8

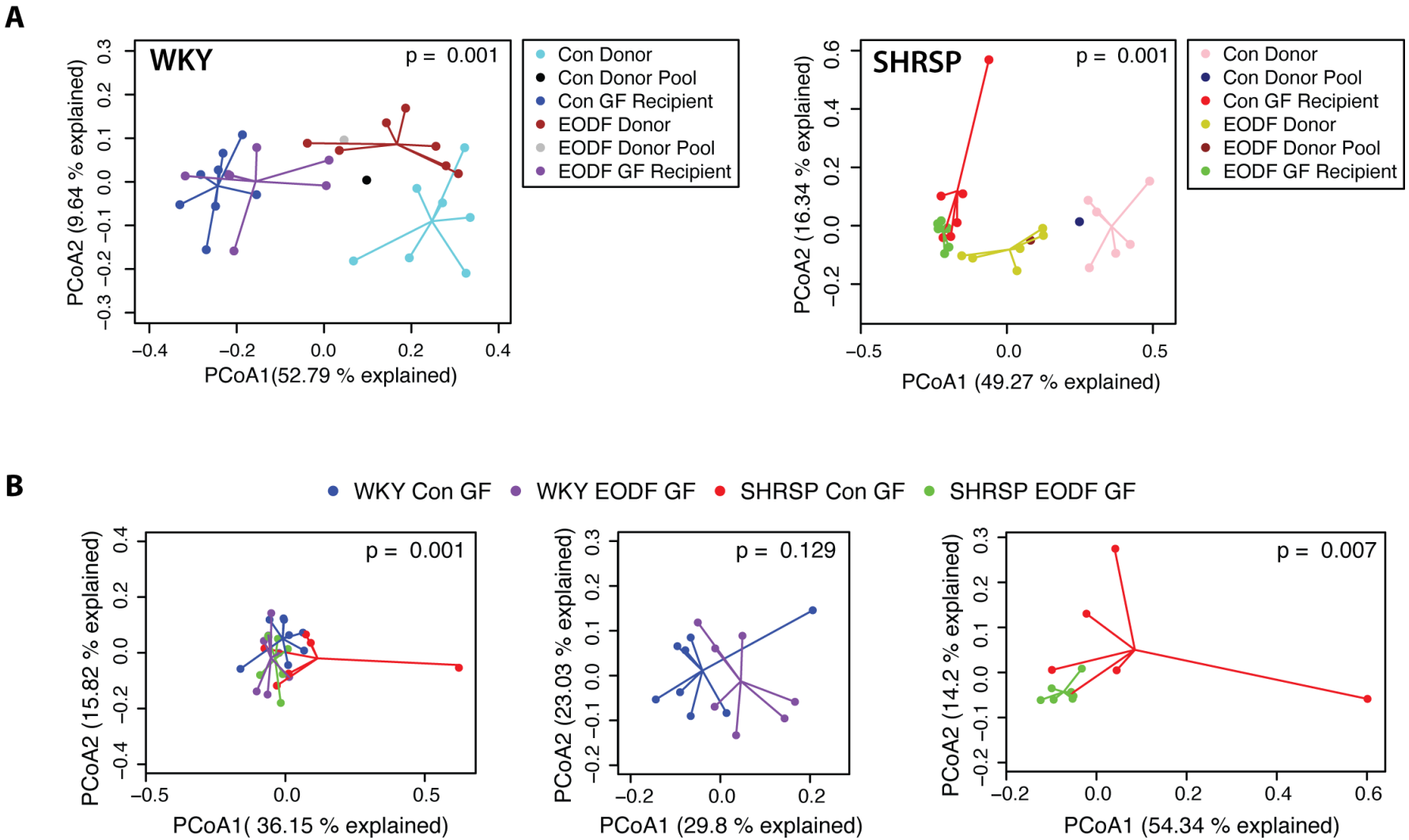

Online Figure II. Beta diversity of donors and GF recipients in FMT study. Principal Coordinate Analysis plots of Bray-Curtis dissimilarity of **(a)** donors, pooled cecal content, and GF recipients of WKY (left) and SHRSP (right), and of **(b)** four transplanted GF groups (left), GF WKY recipients (middle), and GF SHRSP recipients(right). n=6-8

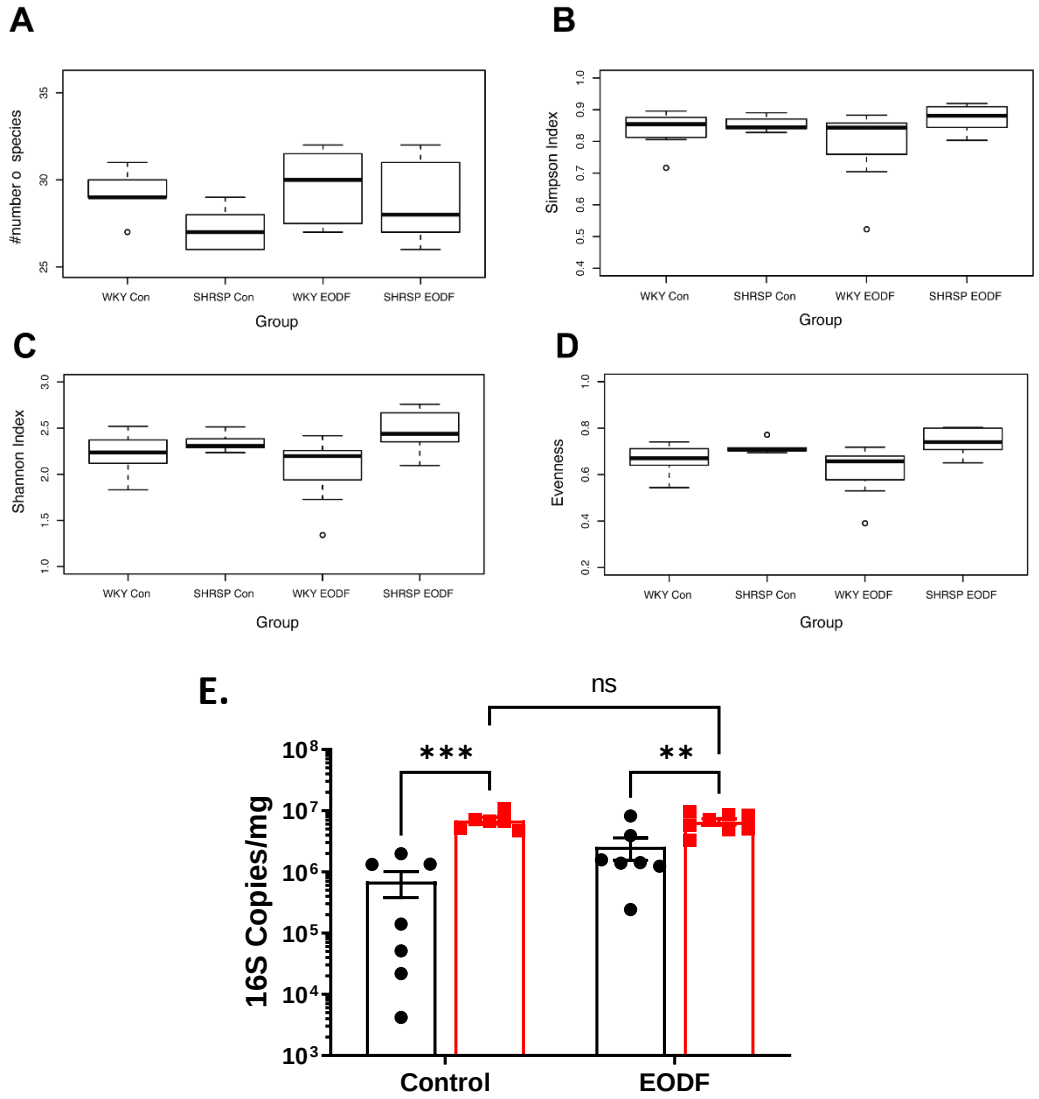

Online Figure III. EODF alters the microbial makeup of WKY and SHRSP gut microbiota. (a) Richness **(b)** Simpson Diversity, **(c)** Shannon Diversity indices of alpha diversity **(d)** Evenness and **(e)**bacterial load. Data presented as mean ± SEM. Two-way ANOVA with robust estimator followed by Mann-Whitney U test with Benjamin-Hochberg *post hoc* correction (a-d). Two-way ANOVA with Tukey's multiple comparisons test (e). **p=0.0054, ***p =0.0001, n=6-8.

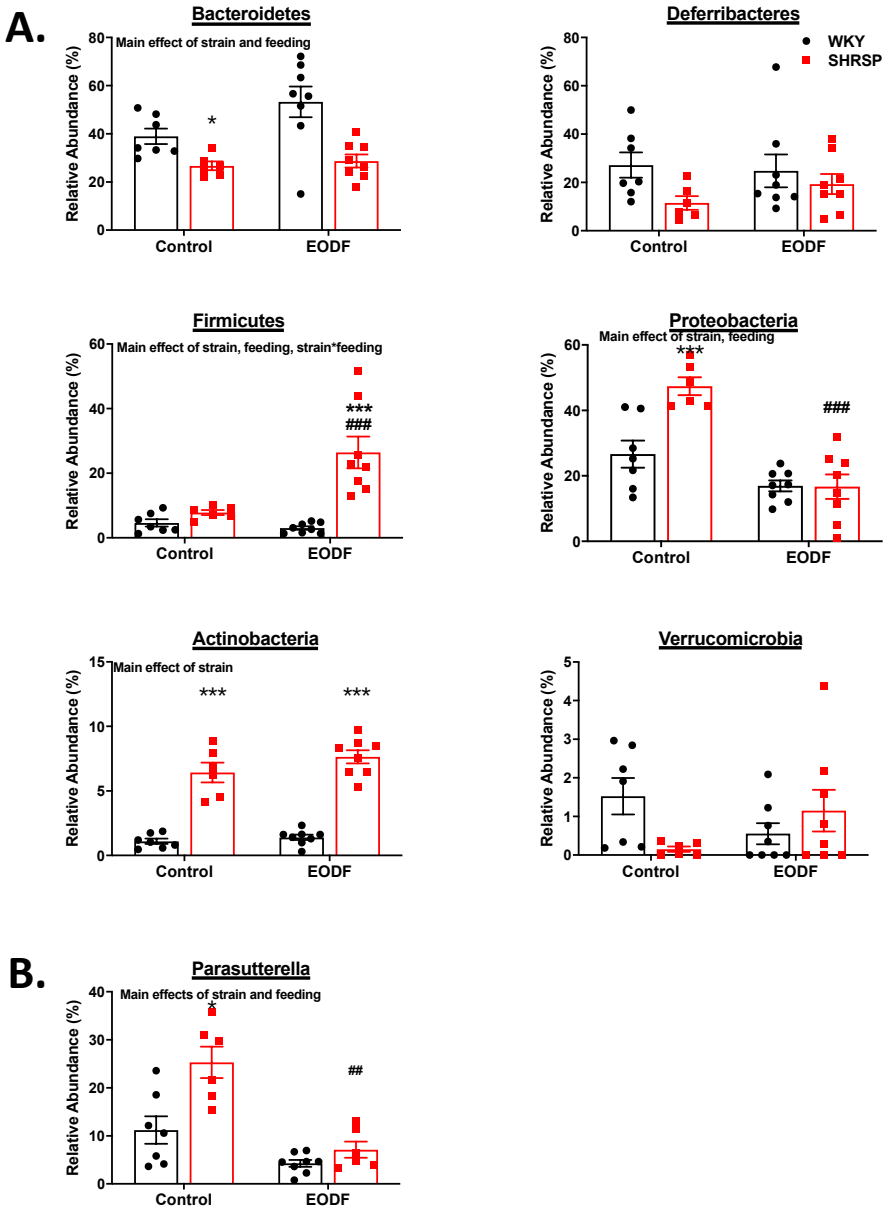

Online Figure IV. Strain and EODF alter the makeup of the gut microbiota. Effects of strain and EODF on phyla **(a)** and genus *Parasutterella* **(b)**. Data presented as mean ± SEM. Two-way ANOVA with robust estimator followed by Mann-Whitney U test with Benjamin-Hochberg *post hoc* correction. *p≤0.01 vs WKY Con, ***p≤0.005 vs WKY Con, ## p≤0.01 vs SHRSP Con, ###p≤0.005 vs SHRSP Con. n=6-8

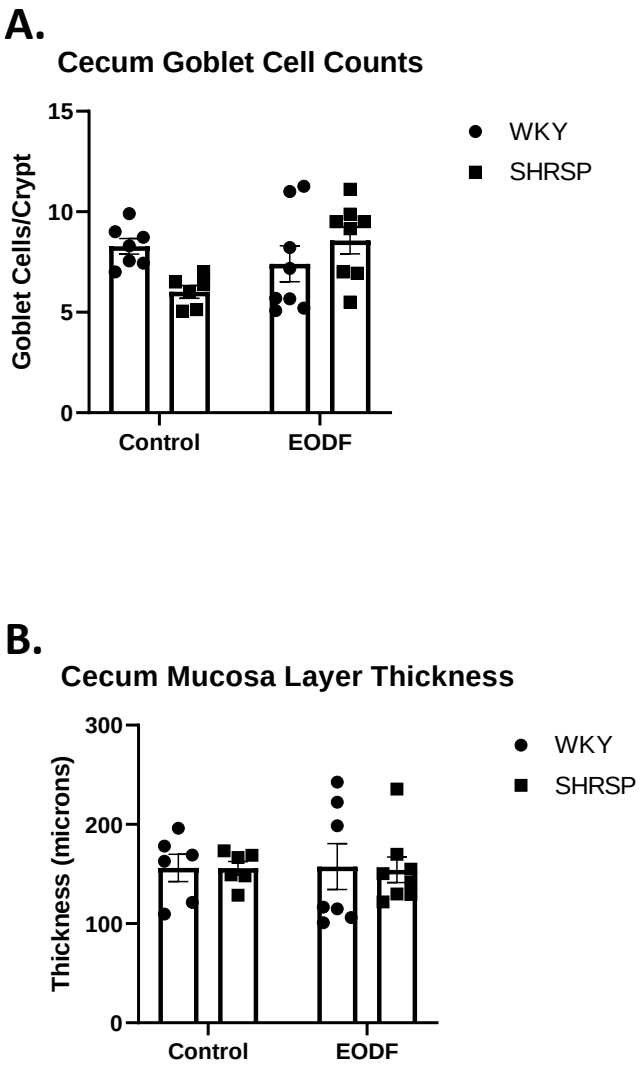

Online Figure V. Local effects of strain and EODF on the gut wall. Cecum goblet cell **(a)** and mucosa layer thickness **(b)**.

C.

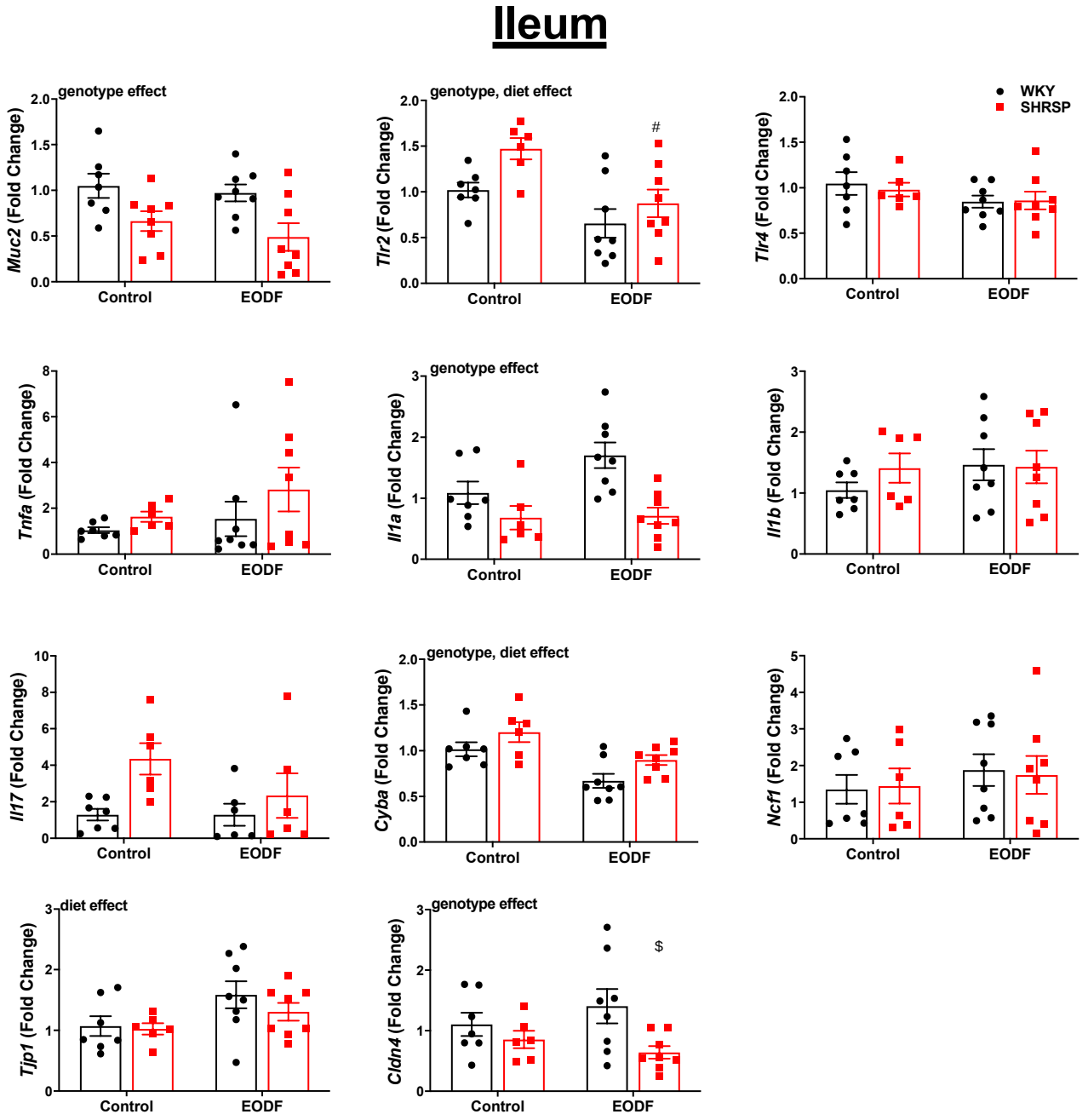

Online Figure V. Local effects of strain and EODF on the gut wall. Markers of gut wall inflammation and barrier integrity in ileum **(c)**

D.

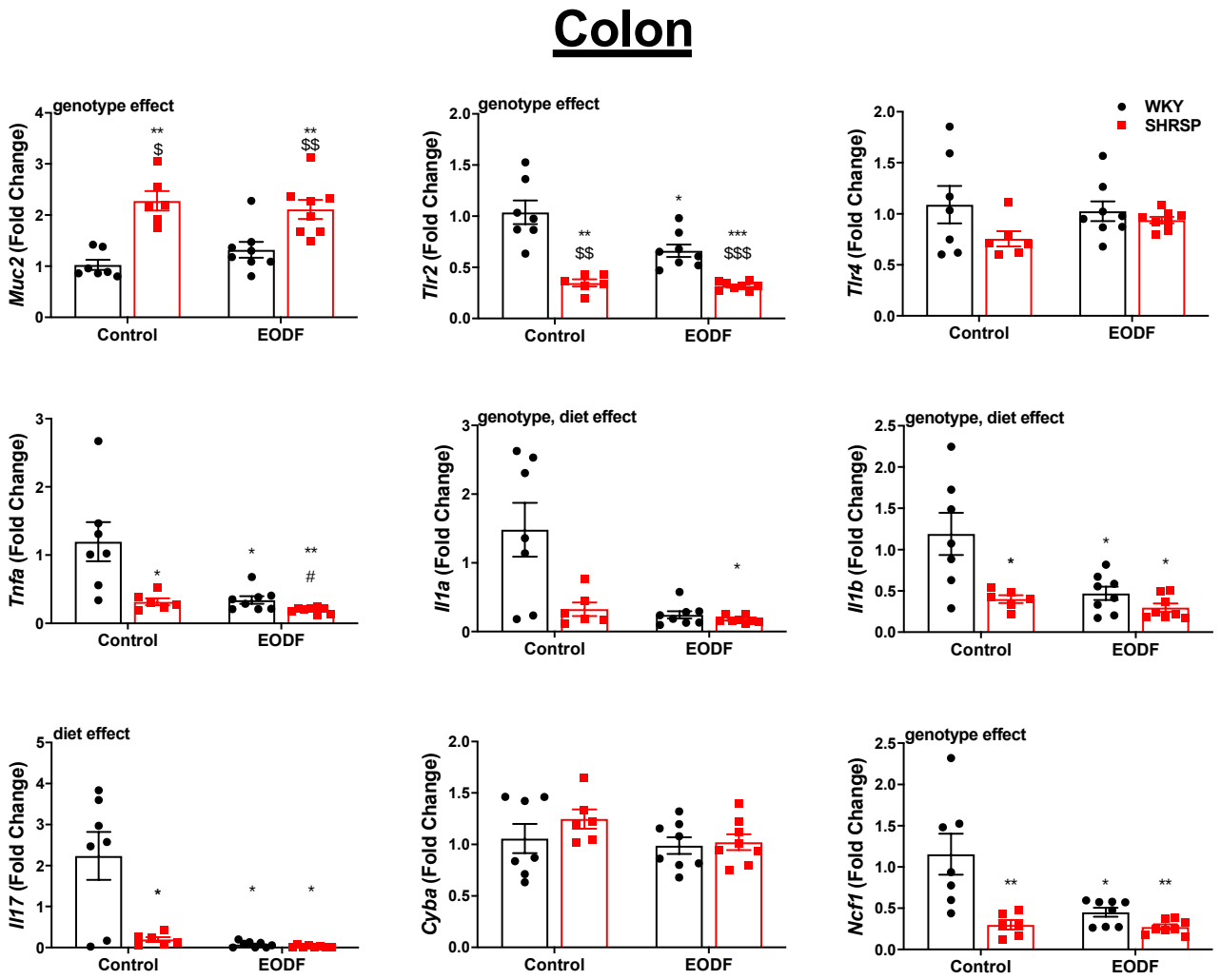

Online Figure V. Local effects of strain and EODF on the gut wall. and colon **(d)**. All genes normalized to *Hprt* expression. Two-way ANOVA with Tukey's multiple comparisons test or two-way ANOVA with robust estimator followed by Mann-Whitney U test with Benjamin-Hochberg *post hoc* correction. Main effect of genotype $p \leq 0.0213$ and diet $p \leq 0.0295$. *$p \leq 0.05$ vs WKY Con, **$p \leq 0.01$ vs WKY Con ***$p \leq 0.001$ vs WKY Con, $^{\#}p \leq 0.05$ vs SHRSP Con, $ $p<0.05$ vs WKY EODF, $$ $p<0.01$ vs WKY EODF, $$$ $p<0.001$ vs WKY EODF. n=6-8

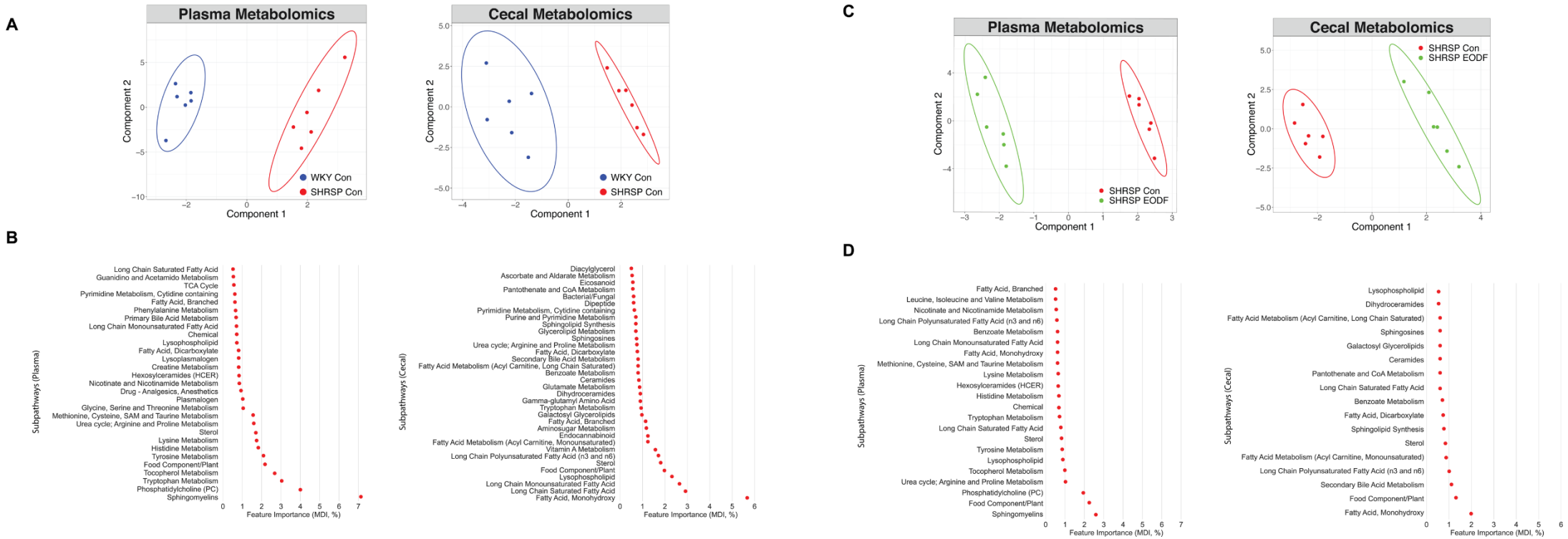

Online Figure VI. Two groups comparison of plasma and cecal metabolites

Plasma and cecal metabolites analysis in control groups (WKY vs SHRSP) **(a)-(b)** and in SHRSP groups (SHRSP Con vs SHRSP EODF) **(c)-(d)**

(a) (c) Sparse partial least squares discriminant analysis (sPLS-DA) of plasma (left) and cecal (right) metabolites

(b) (d) Plasma (left) and cecal (right) metabolite sub pathways identified by random forest classification as important for group separation (Gini index as feature importance).

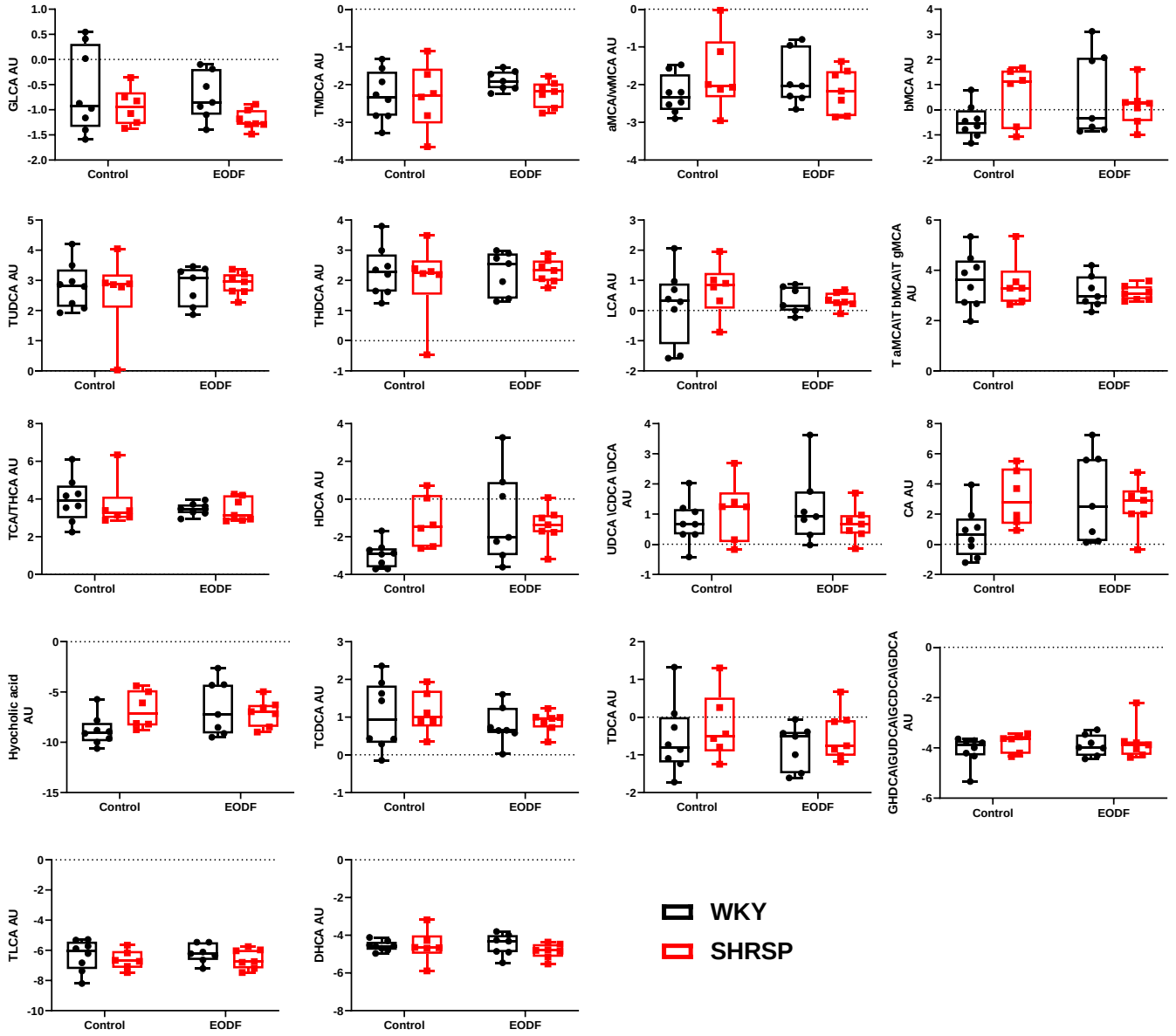

Online Figure VII. Plasma BAs in Transplanted GF Rats. Data are presented as mean±SEM. Two-way ANOVA with Tukey's multiple comparisons test or two-way ANOVA with robust estimator followed by Mann-Whitney U test with Benjamin-Hochberg *post hoc* correction. n=6-8.

	Gene Name	p_interaction	p_genotype	p_treatment	SHRSP Con vs WKY Con	SHRSP Con vs SHRSP EODF
1.1.1.103	L-threonine 3-dehydrogenase	0.94118817	1.63E-05	0.09052858	Significant	Significant
1.1.1.58	Tagaturonate reductase	0.84173275	0.00597159	2.32E-05	Significant	Significant
1.1.1.6	Glycerol dehydrogenase	0.46940516	0.03120857	0.88833094	Significant	Significant
1.17.7.3	(E)-4-hydroxy-3-methylbut-2-enyl-diphosphate synthase (flavodoxin)	0.06468376	0.00023469	0.00220203	Significant	Significant
1.17.98.1	Bile-acid 7-alpha-dehydroxylase	0.00951628	0.08066074	9.22E-06	Significant	Significant
1.17.99.6	Epoxyqueuosine reductase	0.28273452	0.00097706	0.00030322	Significant	Significant
1.2.7.4	Carbon-monoxide dehydrogenase (ferredoxin)	0.03833217	5.43E-05	0.86614155	Significant	Significant
1.3.1.6	Fumarate reductase (NADH)	0.9539988	0.59586438	0.00120937		Significant
1.3.1.74	2-alkenal reductase (NAD(P)(+))	5.94E-05	3.47E-07	1.86E-05		Significant
1.4.1.3	Glutamate dehydrogenase (NAD(P)(+))	0.63402971	6.30E-06	0.05352955	Significant	Significant
1.5.1.39	FMN reductase (NAD(P)H)	0.81637828	5.56E-06	0.0334371	Significant	Significant
1.8.4.14	L-methionine (R)-S-oxide reductase	0.89517575	4.21E-05	0.20795832	Significant	Significant
1.9.6.1	Nitrate reductase (cytochrome)	0.60378568	0.0089968	0.00478045		Significant
2.1.1.171	16S rRNA (guanine(966)-N(2))-methyltransferase	0.03906394	0.00171274	0.01531347	Significant	Significant
2.1.1.185	23S rRNA (guanosine(2251)-2'-O)-methyltransferase	0.61765196	0.10339482	0.03391295		Significant
2.1.1.198	16S rRNA (cytidine(1402)-2'-O)-methyltransferase	0.32693563	0.0155832	4.01E-06		Significant
2.1.1.199	16S rRNA (cytosine(1402)-N(4))-methyltransferase	0.02188012	0.00618412	0.00015282	Significant	Significant
2.1.1.201	2-methoxy-6-polyprenyl-1,4-benzoquinol methylase	0.83417176	0.02879082	0.0174588		Significant
2.1.1.80	Protein-glutamate O-methyltransferase	0.10960987	0.32297735	0.04508349		Significant
2.3.1.47	8-amino-7-oxononanoate synthase	0.55927754	1.23E-05	0.0596068	Significant	Significant
2.3.1.61	Dihydrolipoyllysine-residue succinyltransferase	0.68804952	0.24921357	0.00240873		Significant
2.3.1.81	Aminoglycoside N(3')-acetyltransferase	0.77453039	0.00027549	0.00720042		Significant
2.4.1.212	Hyaluronan synthase	0.77537352	5.69E-06	0.01536576	Significant	Significant
2.4.1.250	D-inositol-3-phosphate glycosyltransferase	0.57105432	2.48E-05	0.02797384	Significant	Significant
2.4.2.43	Lipid IV(A) 4-amino-4-deoxy-L-arabinosyltransferase	0.78068133	0.00017137	0.55971049	Significant	Significant
2.4.2.9	Uracil phosphoribosyltransferase	0.01300093	0.03752991	0.32783833	Significant	Significant
2.5.1.17	Cob(I)yrinic acid a,c-diamide adenosyltransferase	0.64258885	1.37E-06	0.49210207	Significant	Significant
2.5.1.30	Heptaprenyl diphosphate synthase	9.73E-06	0.04658432	0.37713724		Significant
2.6.1.37	2-aminoethylphosphonate--pyruvate transaminase	0.48972389	3.05E-06	0.00026462	Significant	Significant
2.6.1.87	UDP-4-amino-4-deoxy-L-arabinose aminotransferase	0.98650538	1.02E-05	0.04918729	Significant	Significant
2.7.1.15	Ribokinase	0.0036223	0.00515885	0.02352536	Significant	Significant
2.7.1.168	D-glycero-alpha-D-manno-heptose-7-phosphate kinase	0.16746475	0.40008456	0.04351392		Significant
2.7.1.25	Adenylyl-sulfate kinase	0.40939194	9.88E-07	0.03371321	Significant	Significant
2.7.1.55	Allose kinase	0.9104841	0.22996218	0.01598217		Significant
2.7.14.1	Protein arginine kinase	0.02217065	0.7889024	0.08499409	Significant	Significant

2.7.2.1	Acetate kinase	0.06470757	0.34825611	0.00071586		Significant
2.7.2.11	Glutamate 5-kinase	0.81680953	0.01966005	9.73E-05		Significant
2.7.2.4	Aspartate kinase	0.34872864	0.00020064	0.0272182		Significant
2.7.4.25	(d)CMP kinase	0.08231094	0.00272472	0.00050527	Significant	Significant
2.7.4.3	Adenylate kinase	0.0360737	0.02628479	0.01433446	Significant	Significant
2.7.7.4	Sulfate adenylyltransferase	0.18712076	1.25E-05	0.06324455	Significant	Significant
2.7.7.42	[Glutamate--ammonia-ligase] adenylyltransferase	0.48590141	0.39019122	0.01634703		Significant
2.7.7.43	N-acylneuraminate cytidylyltransferase	0.01204108	0.11874134	0.01211516		Significant
2.7.7.59	[Protein-PII] uridylyltransferase	0.43076749	0.52061543	0.03809492		Significant
2.7.7.65	Diguanylate cyclase	0.66005041	0.0485028	0.98309723	Significant	Significant
2.7.7.81	Pseudaminic acid cytidylyltransferase	0.75223966	0.00127678	3.64E-05		Significant
2.7.7.89	[Glutamate--ammonia ligase]-adenylyl-L-tyrosine phosphorylase	0.29177345	0.90703742	0.01248102		Significant
2.7.8.26	Adenosylcobinamide-GDP ribazoletransferase	0.88640877	7.83E-08	0.01238049	Significant	Significant
2.7.9.3	Selenide, water dikinase	0.0409356	7.07E-05	0.68553321	Significant	Significant
2.8.1.13	tRNA-uridine 2-sulfurtransferase	0.18916384	0.00423478	0.00544074	Significant	Significant
2.8.1.7	Cysteine desulfurase	0.00664508	0.65149945	0.00761682		Significant
2.8.3.1	Propionate CoA-transferase	0.00480949	0.01594618	0.00026751		Significant
2.8.3.12	Glutaconate CoA-transferase	0.02763692	0.0302324	0.00499009	Significant	Significant
3.1.1.11	Pectinesterase	0.75489462	0.03433685	0.00077029	Significant	Significant
3.1.11.2	Exodeoxyribonuclease III	0.17432764	0.00033069	0.00135452	Significant	Significant
3.1.26.12	Ribonuclease E	0.49206887	0.12932148	0.03959749		Significant
3.1.26.4	Ribonuclease H	0.00010867	0.0058745	0.43103636	Significant	Significant
3.1.3.48	Protein-tyrosine-phosphatase	0.03867096	0.00012516	0.75675495	Significant	Significant
3.1.6.1	Arylsulfatase	0.38972548	8.55E-06	0.17471212	Significant	Significant
3.2.1.10	Oligo-1,6-glucosidase	3.50E-05	0.03505446	0.40129956	Significant	Significant
3.2.1.103	Keratan-sulfate endo-1,4-beta-galactosidase	0.06710298	0.1085898	0.00292295		Significant
3.2.1.14	Chitinase	0.63854524	1.03E-05	0.05997925	Significant	Significant
3.2.1.180	Unsaturated chondroitin disaccharide hydrolase	0.02227623	0.03430809	0.18697953	Significant	Significant
3.2.1.51	Alpha-L-fucosidase	0.9958628	2.80E-05	0.11828038	Significant	Significant
3.2.1.73	Licheninase	0.69812776	2.04E-06	0.23031855	Significant	Significant
3.2.1.78	Mannan endo-1,4-beta-mannosidase	0.32281901	0.00195163	0.01017243	Significant	Significant
3.2.2.27	Uracil-DNA glycosylase	0.4934377	0.52233389	0.00412549		Significant
3.2.2.8	Ribosylpyrimidine nucleosidase	0.93487966	0.00462057	0.1275953	Significant	Significant
3.3.1.1	Adenosylhomocysteinase	0.00828116	0.01607177	0.19641002	Significant	Significant
3.4.11.18	Methionyl aminopeptidase	0.00807899	0.09308523	0.00014321	Significant	Significant
3.4.13.22	D-Ala-D-Ala dipeptidase	0.73259949	2.67E-05	0.00092194	Significant	Significant

3.4.14.5	Dipeptidyl-peptidase IV	0.59598541	3.39E-05	0.05318218	Significant	Significant
3.4.15.5	Peptidyl-dipeptidase Dcp	0.40327662	2.29E-06	0.95984504	Significant	Significant
3.4.21.102	C-terminal processing peptidase	0.65727899	9.28E-06	0.2242036	Significant	Significant
3.4.21.108	HtrA2 peptidase	0.40044039	2.06E-05	0.05638295	Significant	Significant
3.5.1.16	Acetylornithine deacetylase	0.41953812	3.85E-06	0.65210478	Significant	Significant
3.5.1.2	Glutaminase	0.62061719	8.16E-07	0.00014013	Significant	Significant
3.5.1.25	N-acetylglucosamine-6-phosphate deacetylase	0.00671805	0.00913843	0.11763424	Significant	Significant
3.5.1.5	Urease	0.11690786	0.29123281	0.00035274		Significant
3.5.4.2	Adenine deaminase	0.02646604	0.05525354	0.00942029	Significant	Significant
3.5.4.28	S-adenosylhomocysteine deaminase	0.03418805	0.23786196	0.04706119		Significant
3.5.4.30	dCTP deaminase (dUMP-forming)	0.94127675	0.00604087	2.73E-05	Significant	Significant
3.5.4.31	S-methyl-5'-thioadenosine deaminase	0.01585857	0.22249889	0.0409682	Significant	Significant
3.5.4.4	Adenosine deaminase	0.12836811	0.20703717	0.0173345		Significant
3.6.1.41	Bis(5'-nucleosyl)-tetraphosphatase (symmetrical)	0.00704132	0.08136704	0.00030304		Significant
3.6.1.57	UDP-2,4-diacetamido-2,4,6-trideoxy-beta-L-altropyranose hydrolase	0.14097986	0.1806252	0.00035815	Significant	Significant
3.6.1.66	XTP/dITP diphosphatase	0.1308931	0.03313838	0.00200423		Significant
3.6.3.15	Sodium-transporting two-sector ATPase	0.01756682	0.45878066	0.0029734		Significant
3.6.3.17	Monosaccharide-transporting ATPase	0.12337794	0.08998702	0.04395567	Significant	Significant
3.6.3.29	Molybdate-transporting ATPase	0.64492847	0.00185127	0.00721782		Significant
3.6.3.41	Heme-transporting ATPase	0.21550434	0.00061684	0.86183623	Significant	Significant
4.1.2.25	Dihydroneopterin aldolase	0.3862489	5.27E-05	0.00107656	Significant	Significant
4.2.1.1	Carbonate dehydratase	0.71862136	1.16E-06	0.06285503	Significant	Significant
4.2.1.115	UDP-N-acetylglucosamine 4,6-dehydratase (inverting)	0.03308045	0.60221693	0.00056587	Significant	Significant
4.2.1.53	Oleate hydratase	0.0768188	0.60213499	0.00322456		Significant
4.6.1.1	Adenylate cyclase	0.8607175	0.00021241	0.11691791	Significant	Significant
5.1.1.3	Glutamate racemase	0.04420112	0.00302542	0.00214567		Significant
5.1.1.7	Diaminopimelate epimerase	0.16804105	0.00129077	4.31E-05		Significant
5.1.3.14	UDP-N-acetylglucosamine 2-epimerase (non-hydrolyzing)	0.79444817	5.02E-06	0.04575206	Significant	Significant
5.1.3.32	L-rhamnose mutarotase	0.26458811	0.44996126	0.00035742		Significant
5.3.1.14	L-rhamnose isomerase	0.01190756	0.00516245	0.00090398	Significant	Significant
5.4.99.26	tRNA pseudouridine(65) synthase	0.49339171	4.49E-05	0.05224734	Significant	Significant
5.4.99.28	tRNA pseudouridine(32) synthase	0.60397514	1.12E-05	0.1176687	Significant	Significant
5.99.1.2	DNA topoisomerase	0.00301764	0.50088529	1.59E-05		Significant
6.1.1.16	Cysteine--tRNA ligase	4.21E-05	0.36332712	0.00324354	Significant	Significant
6.1.1.21	Histidine--tRNA ligase	0.00144515	0.00268136	0.02522565	Significant	Significant
6.1.1.7	Alanine--tRNA ligase	0.02231194	0.00046723	0.139446	Significant	Significant

6.3.2.2	Glutamate--cysteine ligase	0.00096377	0.30341452	0.16470851		Significant
6.3.5.4	Asparagine synthase (glutamine-hydrolyzing)	0.42022732	0.13146755	2.04E-05	Significant	Significant
6.5.1.2	DNA ligase (NAD(+))	0.01167422	0.2438767	0.05930332		Significant